*Journal of Structural Chemistry. Vol. 58, No. 5, pp. 1009-1017, 2017.*


# CHEMICAL ASPECT OF THE STRUCTURAL DISORDER IN $CuCrS_2$ AND $CuCr_{1-x}V_xS_2$ SOLID SOLUTIONS

**I. G. Vasilyeva**

UDC 541.221:546.56+546.76

A gradient chemical structure of micron-sized crystals of $CuCrS_2$ and $CuCr_{1-x}V_xS_2$ powders is established by the differential dissolution technique. It is shown that their surface region coherently conjugated with planar faces of $CuCrS_2$ crystals is enriched with copper whereas the bulk is depleted of copper and the copper sublattice is disordered. A possible mechanism of the formation of surface regions due to a high bulk mobility of copper atoms in the defect copper sublattice is proposed. It is shown that for solid solutions the disordering process involves copper and vanadium atoms and vacancy complexes. The phenomena found are discussed together with the structural and magnetic data.

**DOI:** 10.1134/S0022476617050225

**Keywords:** quaternary copper-chromium-vanadium sulfide, chemical heterogeneity, disordering, phase transitions.

## INTRODUCTION

The layered compound $CuCrS_2$ and its solid solutions $CuCr_{1-x}V_xS_2$ have long been considered as promising multifunctional materials for modern electronics [1-3]. The necessity to understand and explain the specific electrical and magnetic properties of these objects has started an extensive investigation of their structural and chemical states. However, the scatter of physical properties altering from a sample to sample being macroscopically identical proved to be so serious that the statement that the properties of an object depended on its preparation conditions became inacceptable for the materials science. Two factors gave rise to the main problems of ambiguity in the interpretation of microstructure–property correlations. These are the absence of quality crystals with a size sufficient for large-scale studies and a set of diagnostic techniques restricted by the powder state of the objects. The specific features of the layered compound itself also contributed to the ambiguity. Many researchers considered it as an intercalate of a small $Cu^+$ ion in tetrahedral voids of the space between $[CrS_2]^-$ layers of the matrix structure. In fact, the bond between positively charged $Cu^+$ layers and negatively charged $[CrS_2]^-$ layers is not purely electrostatic but there is a strong salt-type interaction between interlayer copper atoms and sulfur from S–Cr–S layers, which at high temperatures predetermines the disordering process of the copper sublattice.

A large number of works have been devoted to the study of structural disordering of powder $CuCrS_2$ samples and $CuCr_{1-x}V_xS_2$ solid solutions by powder X-ray diffraction, neutron diffraction, X-ray emission spectroscopy and measurements of the electrical and magnetic properties [1-12]. Despite a large factographic material the final conclusion about the character of the copper distribution in the matrix compound $CuCrS_2$ and the vanadium distribution in the $CuCr_{1-x}V_xS_2$ solid solution

Nikolaev Institute of Inorganic Chemistry, Siberian Branch, Russian Academy of Sciences, Novosibirsk; kamarz@niic.nsc.ru. Translated from *Zhurnal Strukturnoi Khimii*, Vol. 58, No. 5, pp. 1047-1055, June-July, 2017. Original article submitted January 12, 2017.

has not been drawn so far. Some researchers consider $CuCr_{1-x}V_xS_2$ to be a substitutional solid solution, the others consider it to be a substitution-intercalation solution, indicating that vanadium can occupy irregular octahedral voids of the $CuCrS_2$ interlayer space.

Powder X-ray diffraction, neutron diffraction, X-ray absorption and photoelectron spectroscopy methods would seem to provide these data and discriminate between different models of the structure. However, in practice, with regard to limitations of each of these methods when applied to disperse sized powders with a violated surface state and a long interface, the unambiguous structure solution of both matrix and solid solutions, which is consistent with the specific features of the measured electrical and magnetic properties, has not been obtained so far. This is facilitated by the fact that as the distribution of copper and vanadium is complicated in $CuCrS_2$ and $CuCr_{1-x}V_xS_2$, the ordering process starts to involve vacancies in copper and chromium layers, which predetermines an intricate ordering process with several degrees of order.

The necessity of understanding the order–disorder process in $CuCrS_2$ and $CuCr_{1-x}V_xS_2$ solid solutions forced us to return to this problem and develop new approaches to its solution. To examine the fine structure of a series of $CuCrS_2$ and $CuCr_{1-x}V_xS_2$ samples we have chosen an independent chemical method of differential dissolution (DD) [13]. The targeted choice of the DD method is based on its ability to precisely determine the phase composition and stoichiometry of the matrix and impurity phases, but its major advantage is the opportunity to monitor the spatial chemical heterogeneity with a resolution of 50 Å/cm$^2$ and to determine the concentration of diffusively mobile ions in the structure by its specific reactivity [7]. This work is devoted to the development of representations of the nature of disordering in these interesting layered compounds that are two-dimensional in the structure and properties, with the attention focused on the chemical aspect of the problem. We were sure that the analysis of chemical DD spectra correlated with the structural data on possible models of $CuCrS_2$ and $CuCr_{1-x}V_xS_2$ structures, contributing to the available knowledge about these objects, would provide new and more complete information on the phenomenon under study.

## EXPERIMENTAL

The object of study was a series of samples of micron-sized powders of the composition $CuCrS_2$ and $CuCr_{1-x}V_xS_2$ with $x = 0 \div 0.6$ that were obtained by sulfurizing a stoichiometric mixture of copper, chromium, and vanadium oxides in a gas medium of decomposition products of ammonium rhodanide. In their synthesis, gradual heating of the mixture was applied which ensured the completeness of the final product formation. The key parameters of the synthesis were five hour heating at a final temperature of 850 °C and cooling to room temperature with a rate of 25 °C/min or 60 °C/min. The grained composition of the samples was found to be 1-25 μm with the preferred concentration of the micron fraction. We and other researchers have previously studied in detail these samples within the international project [14]. However, the DD data were not published because they did not principally influence the main conclusions. Since the question about the disorder of $CuCrS_2$ and $CuCr_{1-x}V_xS_2$ structures still remains a topic of discussions, here we consider it from a new standpoint, focusing our attention on the chemical aspect of the problem of disorder and measuring the magnetic properties of the samples. We used the structural data previously obtained by T. Yu. Kardash [14] to support the representations being developed.

DD was performed in the $HNO_3$ solvent with increasing concentration from 3N to 6N at temperatures of 20-80 °C. The samples were completely dissolved in 25-30 min, except $Cr_2O_3$ grains remaining on the reactor walls after the completion of dissolution. The initial information was the kinetic dissolution curves of elements composing the sample, which were transformed into stoichiograms and the stoichiometric formulas of phases and their quantities were calculated. A detailed description of all procedures is given in [13].

The magnetic properties of $CuCr_{1-x}V_xS_2$ were measured on a magnetic balance according to the Faraday scheme at temperatures of 80-300 K and the magnetic field power of ~1 T (10 kOe).

The methods of examining the structure are described in detail in [7, 14]. Here we present only brief information on the measurement conditions. The measurements were conducted on an X′TRA diffractometer with Cu$K_\alpha$ radiation in the angle range $2\theta$ = 10-70° (the interval of reflections with $I/I_0 \geq 1\%$) with a step of 0.02° and the point acquisition time of 5 s.

The crystal structure was refined by the full-profile analysis using the GSAS program; the PCW program was employed to refine the lattice parameters, to reveal the copper and vanadium sites and their occupancy factors.

## RESULTS AND DISCUSSION

The dissolution process of the $CuCrS_2$ powder in the 3N $HNO_3$ → 6N $HNO_3$ solvent, 25 °C → 80 °C is depicted in Fig. 1 as the kinetic dissolution curves of Cu, Cr, and S elements and these dissolution curves were recalculated into the kinetic curves using the calculation procedures of the DD technique [13]. The curve profile demonstrates the dissolution of a single-phase sample which proceeds in three stages. The first stage is the exchange reaction of mobile lattice copper ions with solvent protons, which occurs without destructing the matrix structure: $CuCrS_2(s) + H^+(aq) \rightarrow Cu^+(aq) + H_zCu_{1-z}CrS_2(s)$. The matrix itself dissolves under more severe conditions with the two-stage bond cleavage: the crystal surface dissolves first, with copper and sulfur atoms passing into the solution, and then the bulk dissolves, with copper, chromium, and sulfur ions being detected there.

The evident variability of the Cr/Cu atomic ratio during the complete dissolution of the sample determines its spatial chemical heterogeneity, where the surface is substantially enriched with copper as compared to the bulk. A complex profile of the kinetic dissolution curve of the surface means the occurrence of grains with different sizes and morphologies in the powder which dissolve with different rates. The found chemical composition of the sample with the atomic ratio of elements Cu:Cr:S = 1.0:1.01:2.03 reflects its stoichiometry, and the dissolution curve profiles of the elements show its single-phase state. At the same time, the three components of the sample differ from each other in copper nature and its concentration determined by the area of the respective peak. These are lattice/exchange copper (~1 wt.%), surface copper (17%), and bulk copper ( 80%). The bulk composition is determined by the formula $Cu_{0.58}CrS_2$ (error 15%), it is depleted of copper, and the total charge balance of the crystal is provided by mobile lattice and surface copper ions as the components of the whole. It is worth noting that the copper enriched surface of composition gradient crystals has a structure different from the structure of the copper-deficient bulk saturated with non-equilibrium vacancies.

In [7] different copper types identified by DD during the dissolution of $CuCrS_2$ were correlated with the distinction in their crystallographic environment together with the results of powder X-ray diffraction. In the consideration of possible structural models it was established that especially mobile copper atoms were located in the interlayer *o*-positions of octahedra with interatomic Cu–S(1) and Cu–S(2) distances of 2.74-2.63 Å while the rigidly bound copper ions were located in α-positions of tetrahedra with distances of 2.20-2.42 Å and without the diffusion mobility.

The complete disorder in the $CuCrS_2$ structure is known to be not quenched, however, it is very difficult to achieve the complete ordering where α-positions are half-filled [15, 16]. With a part of copper atoms in the octahedra, the $CuCrS_2$ phase seems to be partially ordered, and from the thermodynamic standpoints it is unstable and capable of aging. In [7] it is shown that under artificial aging conditions (on heating to 500 °C) the copper atoms are located in the irregular *o*-positions to

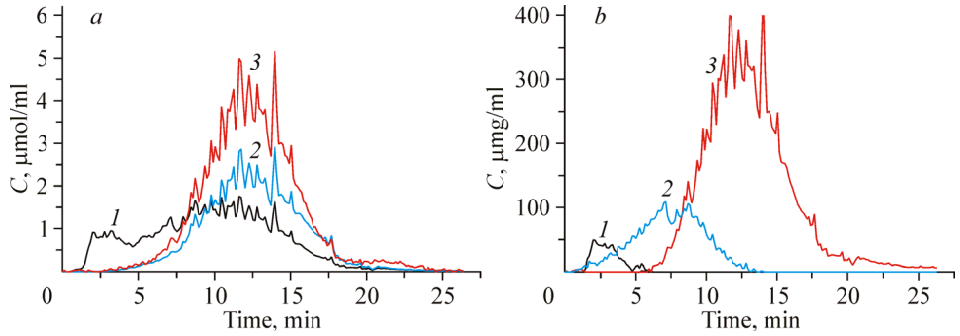


**Fig. 1.** Kinetic dissolution curves of Cu (*1*), Cr (*2*), S (*3*) elements (*a*); components Cu mobile (*1*), surface (*2*), bulk (*3*) (*b*).

form a new $Cu_9S_5$ phase, without changing the matrix lattice symmetry and parameters. The fact of the $Cu_9S_5$ phase formation and the DD data on the gradient chemical structure of the grains give grounds to believe that the bulk diffusion motion of copper ions due to a high degree of defectiveness of the $CuCrS_2$ structure are responsible for the stability of the $CuCrS_2$ structure and the main parameters of its solid phase transformations for thermal action. To prove the reality of this idea we analyzed the features of the $CuCrS_2$ structure.

Fig. 2 shows the arrangement of tetrahedral and α, β and octahedral copper *o*-positions in the rigid three-dimensional framework of $CuCrS_2$ where the number of vacant copper sites exceeds the number of its ions. Here the octahedra are special structural sites where copper distributed with a low density can move fast along diffusion channels formed by the neighboring octahedral and tetrahedral voids in the interlayer space. In [17] the presence of this type of diffusion channels was found experimentally for silver ions in the $AgCrS_2$ phase being an isostructural analogue of $CuCrS_2$. The fact of a high mobility of octahedral copper ions responsible for superionic conductivity was established in [4, 15], where its mobility was determined to be equal to the mobility of typical electrolyte ions. All this enables the consideration of the dynamics of the octahedral copper motion in a solid at a fluid level rather than harmonic vibrations of the crystal lattice.

The peculiarity of diffusion processes in the $CuCrS_2$ structure is also supported by the powder X-ray diffraction analysis that we carried out earlier [7]. In the proposed model of disordering of the copper sublattice with $R_p = 5.1\%$ and $wR_p = 7.5\%$ the thermal atomic parameters of copper in the octahedra were found to be very high relative to other atoms, which indicates the tendency of copper atoms to shift from the central position of the octahedron to faces. The high probability of the acentric location of copper atoms in the octahedra is also confirmed by the EXAFS spectra of $CuCrS_2$, although without calculating these models because of insufficient fitting parameters [8]. The displacement of copper atoms results in the positional disorder and the domain crystal structure due to the copper ability to concentrate in various crystallographic planes of the lattice.

When the $CuCrS_2$ powder is dissolved, the nature of the fast bulk diffusion of copper atoms is manifested in the formation of surface regions with its increased concentration. Following the kinetic curve profiles, these regions do not exist separately and cannot be distinguished in the whole system without changing both composition and structure, as well as characteristics of the bulk part of the matrix associated with them. At the same time, this region is the collective characteristic of the powder surface consisting of many grains where the interface length and properties are distinct for the grains with different sizes, morphology, and surface crystallographic orientation. For the powder with the grain composition of 1-25 μm an approximate estimate of the surface region length is ≤50 nm, and based on the DD data, it should be considered to be a coherent (and semi-coherent) associate conjugated with planar faces of $CuCrS_2$ crystals, which depends on the level of correspondence of their planes to the planes of $Cu_9S_5$ at the interface.

The diffraction pattern of the sample taken from [14] demonstrates that it is single-phase, with the surface state of the crystals being not fixed at all (Fig. 3).

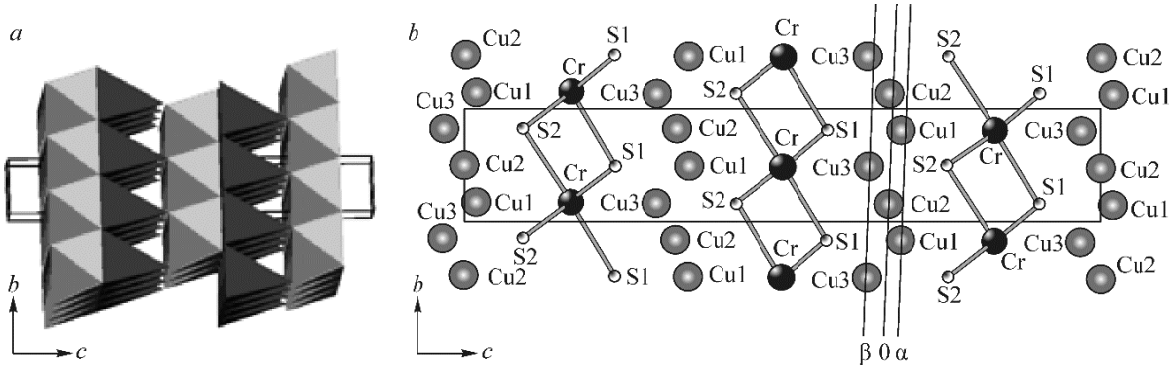


**Fig. 2.** Crystal structure of $CuCrS_2$ along [100] with copper positions.

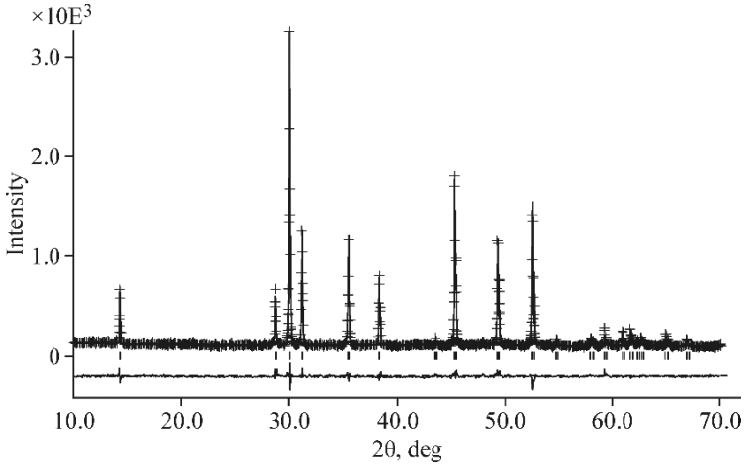


**Fig. 3.** Experimental and difference diffraction patterns of $CuCrS_2$ powder with the 1-25 μm grain composition. Standard parameters: $a$ = 3.481Å, $c$ = 18.720 Å.

However, the results of the structure refinement indicate the presence of copper atoms in the *o*-positions in the amount comparable with the DD data. Other structural data together with the magnetic characteristics of this sample are listed in Table 1.

A low degree of occupancy of the *o*-positions as well as a low concentration of mobile copper give evidence that it is this type of copper atoms that forms the stable surface region where the matrix lattice varies the chemical composition and a minor contraction of the $c$ parameter ($\Delta c$ = 0.02 Å). According to the structural and DD data, the measured Curie temperature Θ and the effective magnetic moment are well consistent with the proposed crystal structure model because the $a$ parameter less than 3.51 Å ensures a stable ferromagnetic state of the chromium layer, although the Cr octahedra are slightly deformed along the $c$ axis. At the same time, an intricate magnetic structure usually observed for $CuCrS_2$ powders [14] is a reflection of the grained structural heterogeneity, which in turn is related to the variability of grain sizes with different lengths of the surface region and the degree of defectiveness of the copper sublattice in the bulk. The ability of copper atoms to be independently distributed over the intra- and interplanar positions of the $CuCrS_2$ structure gives ground to expect structural distinctions in different grains. Note that this phenomenon is real and expected, which is demonstrated by attempts to describe the possible types of the structural disorder of Ag atoms in the $AgCrS_2$ lattice (analogue of $CuCrS_2$) within the pseudospin model (a variant of the Ising model). The calculations yielded 11 equiprobable types of distribution [17].

The occurrence of surface regions enriched with copper is also noted in the dissolution of $CuCr_{1-x}V_xS_2$ powders whose dissolution kinetic curves are similar to those of $CuCrS_2$. As an example, Fig. 4 presents the dissolution kinetic curves of the crystal elements and components, but only for some $CuCr_{1-x}V_xS_2$ samples; the data for all of them are collected in Table 2.

According to the DD data, all indices, such as the profiles of kinetic curves, a large amount of the surface region, strong defectiveness with respect to copper of the bulk of samples with $x$ = 0.4 and 0.6 indicate the absence of a phase with the $CuCrS_2$ structure where the $Cu_9S_6$, $Cu_3VS_4$ phases and decomposition products consisting of vanadium and chromium are

**TABLE 1.** Structural and Magnetic Characteristics of $CuCrS_2$ Powder

| Lattice parameter , Å | Site occupancy | | Magnetic properties |
|---|---|---|---|
| $a$ 3.480 | Cu(1)-α | 0.97 | Θ = –138 K |
| $c$ 18.700 | Cu(2)-*o* | 0.03 | $\mu_B$ = 3.75 μB |
| | Cr(1) | 1.0 | |
| | S(1), S(2) | 1.0 | |

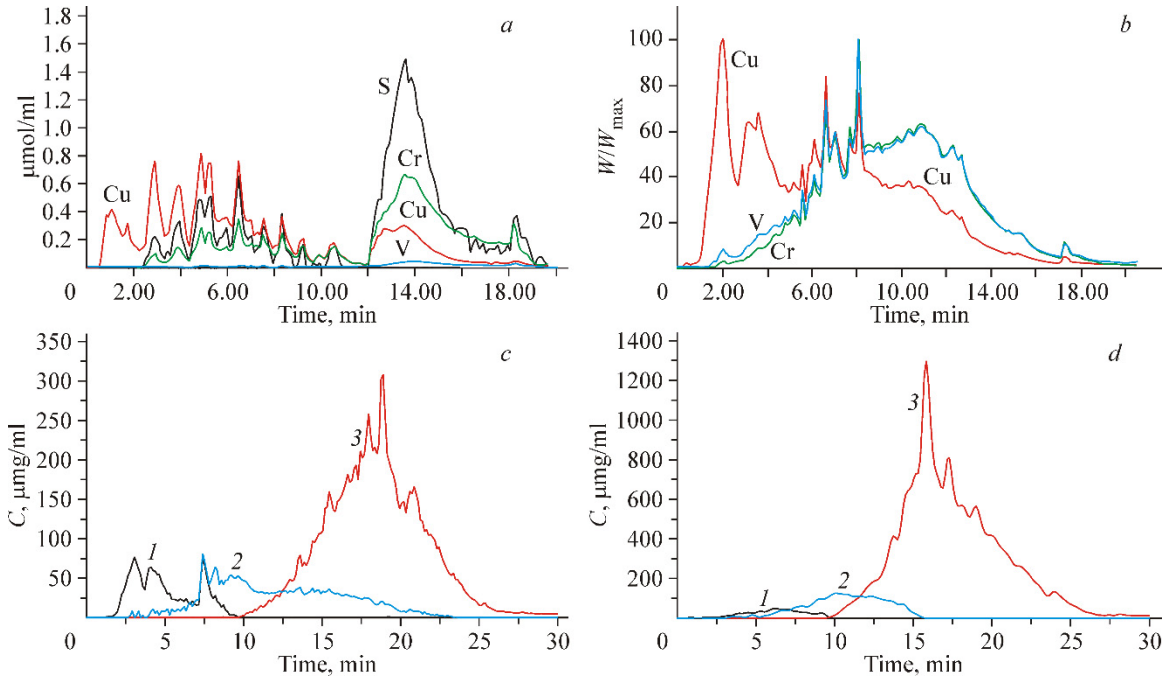


**Fig. 4.** Kinetic dissolution curves of Cu, Cr, V, S elements in $CuCr_{0.85}V_{0.15}S_2$ (*a*) and $CuCr_{0.8}V_{0.2}S_2$ (*b*) samples. Kinetic dissolution curves of $Cu_{mob}$ components (*1*), surface (*2*), bulk (*3*) in $CuCr_{0.80}V_{0.20}S_2$ (*c*) and $CuCr_{0.95}V_{0.05}S_2$ (*d*) samples.

**TABLE 2.** Characteristics of $CuCr_{1-x}V_xS_2$ Samples from the DD Data

| *x* | Cu, wt.% mobile | Surface | | Bulk phase | | Atomic ratio | | | |
|---|---|---|---|---|---|---|---|---|---|
| | | Composition | Concentration, % | Composition | Concentration, % | Cu | Cr | V | S |
| 0 | 3.5 | | 20 | $Cu_{0.59}CrS_2$ | 77 | 60.5 | 61.0 | – | 122 |
| 0.05 | 11 | V:Cu = 0 | 21 | $Cu_{0.39}Cr_{0.95}V_{0.06}S_2$ | 69 | 50.0 | 47.7 | 3.0 | 100 |
| 0.15 | 3 | V:Cu ~ 0.02 | 27 | $Cu_{0.26}Cr_{0.79}V_{0.22}S_2$ | 67 | 86.8 | 79.9 | 8.3 | 168 |
| 0.20 | 3 | V:Cu = 0.037 | 11 | $Cu_{0.23}Cr_{0.80}V_{0.21}S_2$ | 65 | 78.7 | 60.7 | 18 | 157 |
| 0.25 | 3 | V:Cu = 0.040 | 28 | $Cu_{0.21}Cr_{0.75}V_{0.22}S_2$ | 68 | 75.9 | 69.5 | 6.5 | 153 |
| 0.4 | 2 | V:Cu = 0.059 | 30 | $Cu_{0.06}Cr_{0.6}V_{0.4}S_2$ | 70 | 45.6 | 30.5 | 14.8 | 90 |
| 0.6 | | V:Cu ~ 0.33 | 40 | Heterophase sample | | 52.3 | 22.3 | 30.1 | 105 |

detected. Therefore both objects were beyond the scope of our interest. For the samples with $x < 0.4$ with the found chemical stoichiometry the surface and bulk states were discussed in detail. From Table 2 it is seen that the composition of the crystal bulk is depleted of copper, and the larger *x*, the higher this deficit. Together with the copper deficit in the bulk, the length of the surface region enriched with copper increases, and its estimate reaches already 90-100 nm. When sizes exceed the nanoscale size, it is possible to expect a violation of the coherence of surface layers and the appearance of nuclei of the $Cu_9S_5$ phase as colloidal and larger associates, which is detected by weak fluctuations of stoichiograms of the samples with $x < 0.25$ and an additional set of dissolution curves for the samples with $x \geq 0.25$. The removal of the $Cu_9S_5$ phase from the surface region breaks the total stoichiometry and charge neutrality of the sample, thus making the bulk change the composition. Here the non-stoichiometry is compensated by the localization of $V^{3+}$ in the copper sublattice, which is confirmed by two facts: the known ability of chromium atoms to intercalate into the interlayer space [11] and DD vanadium experimentally found in the surface region of the samples with $x \geq 0.15$. The latter fact cannot be explained by anything other than the motion of vanadium atoms from the interlayer *o*-octahedral positions that are fast diffusion channels. The model of localizing vanadium

ions in the interlayer space of the copper sublattice instead of the regular *o*-positions of the chromium layer, which are set by the initial load composition is also supported by the structural data. The diffraction patterns shown in Fig. 5, in which the concentrations of $Cu_9S_5$, $Cu_3VS_4$, and $Cr_2O_3$ impurity phases are determined as 4 wt.%, ~1% wt.%, and ~3-4 wt.% respectively, are taken from [14].

With all limitations of the X-ray diffraction technique and the heterogeneity of these samples, in [14] the reliable results of the structure refinement from the powder X-ray diffraction data were obtained, and we reproduce these data in Table 3.

From the table it is seen that as well as the DD technique, the structural method detects vanadium atoms in the irregular interlayer *o*-positions of the structure, with their concentration decreasing with increasing *x*, which according to the DD data, is due to a high level of its transition from the bulk to the surface layers. These chemical changes maintain the matrix type of the structure but deform the lattice by decreasing the *a* parameter and increasing *c*. The decrease in the *a* parameter can be caused by the appearance of vacancies in the chromium sublattice [$CrS_2$] because vanadium atoms intercalate into the interlayer space rather than occupy these vacancies. The increase in another parameter we associate with the appearance and different positional distribution of vanadium in the interlayer space of the copper sublattice. Our previous X-ray absorption study of the local structure of the $CuCr_{1-x}V_xS_2$ samples with $x = 0.2$ and 0.25 with a detailed analysis of the EXAFS spectra of vanadium atoms has shown that the V *K*-edge XANES spectrum has a feature reflecting its three-dimensional disorder [8]. This fact can be interpreted from the standpoints of the formation of a mixed layered $CuCr_{1-x}V_xS_2$ structure involving the copper and chromium sublattices with different levels of defectiveness whose probability increases when vanadium appears in the composition.

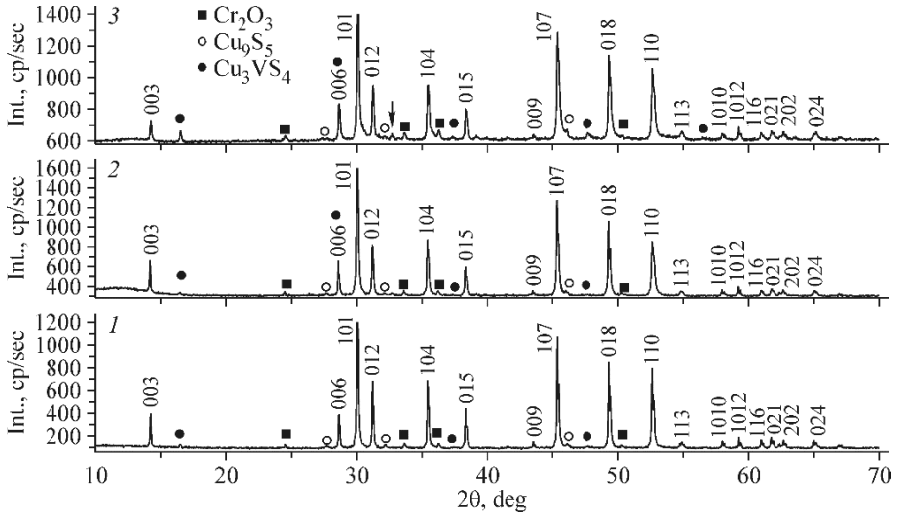


**Fig. 5.** Diffraction patterns of $CuCr_{1-x}V_xS_2$ samples with $x = 0.15$ (*1*), 0.20 (*2*), 0.25 (*3*).

**TABLE 3.** Rhombohedral Cell Parameters and the Site Occupancy Factor in the $CuCr_{1-x}V_xS_2$ Structure

| *x* | 0.15 | | 0.20 | | 0.25 | |
|---|---|---|---|---|---|---|
| Cell parameters, Å | 3.479(1) | 18.696(4) | 3.479(2) | 18.700(3) | 3.4789(2) | 18.699(2) |
| Site occupancy factor | Cu(1)-α | 0.893(5) | Cu(1)-α | 0.891(7) | Cu(1)-α | 0.821(9) |
| | Cu(2)-*o* | 0.107(5) | Cu(2)-*o* | 0.109(7) | Cu(2)-*o* | 0.158(9) |
| | V(1)-*o* | 0.106(8) | V(1)-*o* | 0.09(1) | V(1)-*o* | 0.060(9) |
| | Cr(1), V(2) | 0.894(5) | Cr(1), V(2) | 0.91(1) | Cr(1), V(2) | 0.940(9) |

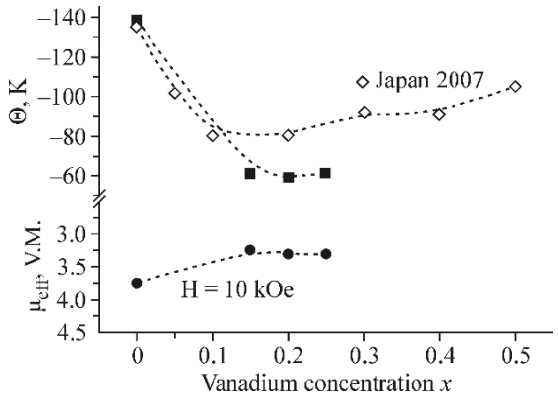


**Fig. 6.** Magnetic characteristics of $CuCr_{1-x}V_xS_2$ samples.

The decrease in the *a* parameter, the appearance of vacancies in the regular positions of the Cr sublattice when vanadium ions move to interstitials affects also the magnetic state of these samples among which only $CuCr_{0.95}V_{0.05}S_2$ is closest to the matrix in structure and composition, according to Table 2. The magnetic properties are illustrated in Fig. 6. On the one hand they support the chemical stoichiometry and charge neutrality of the $Cu^{1+}Cr^{3+}{}_{1-x}V^{3+}{}_xS_2$ samples determined by the chemical DD technique, and on the other hand reflect the found regularities of the grain structure due to the diversity of the crystal structure of different grain volumes. An increase in the areas of the surface region and intergrain boundaries as well as the complex character of copper and vanadium ion distribution in the matrix lattice, which changes from a grain to a grain, also complicates the character and magnetic behavior of the samples.

In accordance with the DD data, Fig. 6 and neutron diffraction results [18] show that only the sample with $x \le 0.1$ retains the matrix symmetry at all temperatures. With increasing doping the coherent magnetic signal is broadened indicating the spin glass state of the other samples.

Thus, the chemical approach developed based on the volumetric experiment conducted by the DD technique proved to be particularly constructive for modeling and understanding the structural disorder of $CuCr_{1-x}V_xS_2$ compounds, which is caused by the specific distribution of mobile copper and vanadium ions. New experimental results revealing the structural features of crystals with the surface enriched with these mobile elements were obtained. Owing to these features the objects themselves turned out to be extremely useful for testing novel chemical approaches developed based on the DD data to get an insight into the structural disorder of compounds.

Since the formation of the final product is set by the thermodynamic and kinetic parameters of the synthesis (temperature, sulfur vapor pressure, and cooling rate), it is the variability of these factors that is the source of diversity of the state of tested objects.

## REFERENCES

1. P. F. Bonger, C. F. Bruggen, J. Koopstra, et al., *J. Phys. Chem. Solids.*, **29**, 977 (1968).
2. F. M. Engelsman, G. Wiegers, F. Jellinek, et al., *J. Solid State Chem.*, **6**, 574 (1973).
3. N. Le Nagard, G. Collin, and O. Gorochov, *Mater. Res. Bull.*, **14**, 1411 (1979).
4. R. F. Almukhametov, R. A. Yakshibaev, E. V. Gabitov, and A. R. Abdullin, *Fiz. Tverd. Tela*, **42**, 1465 (2000).
5. G. M. Abramova, G. A. Petrakovskii, A. M. Vorotynov, and A. N. Velikanov, *Pis'ma v ZhETF*, **83**, 148 (2006).
6. G. M. Abramova, G. A. Petrakovskii, A. N. Vtyurin, et al., *Fiz. Tverd. Tela*, **51**, 500 (2009).
7. I. G. Vasilyeva, T. Yu. Kardash, and V. V. Malakhov, *J. Struct. Chem.*, **50**, No. 2, 288-295 (2009).
8. I. G. Vasilyeva and V. V. Kriventsov, *NIMA*, **4**, 640 (2010).
9. S. V. Titov, A. P. Gorbenko, R. A. Yakshibaev, et al., *Izv. RAN. Ser. Fiz.*, **71**, 743 (2007).
10. G. C. Tewari, T. S. Triathi, and A. K. Rastogi, *Z. Kristallogr.*, **225**, 471 (2010).

11. G. C. Tewari, T. S. Triathi, P. Kumar, et al., *J. Electron. Mater.*, **40**, 2368 (2011).
12. N. Tsujii, H. Kitazawa, and G. Kido, *Phys. Stat. Sol. C*, No. 8, 2775 (2006).
13. V. V. Malakhov and I. G. Vasilyeva, *Usp. Khim.*, **77**, No. 4, 370 (2008).
14. *Report INTAS-SO RAN* № 06-1000013-9002.
15. R. E. Almukhametov, R. A. Yakshibaev, E. V. Gabitov, et al., *Phys. Stat. Sol. B*, **236**, 29 (2003).
16. G. C. Tewari, T. S. Triathi, and A. K. Rastogi, *J. Electron. Mater.*, **39**, 1133 (2010).
17. N. Sharma and T. Tanaka, *Phys. Rev.*, **B28**, 2146 (1983).
18. J. Rash, M. Boehm, J. Schefer, et al., in: *Proc. 16th Int. Conf. Tern. Multinary Comp.*, Berlin (2008), ID 213.